RSC Advances

ROYAL SOCIETY
OF CHEMISTRY

www.rsc.org/advances

Employment of Nanomaterials in Polymerase Chain Reaction: Insight into the Impacts and Putative Operating Mechanisms of Nano-additives in PCR

Meral Yuce, [a]* Hasan Kurt, [b] Venkata R.S.S. Mokkapati, [a] Hikmet Budak [a, b]

[a] Sabanci University, Nanotechnology Research and Application Centre, 34956, Istanbul, Turkey

[b] Sabanci University, Faculty of Engineering and Natural Sciences, 34956, Istanbul, Turkey

Corresponding author: meralyuce@sabanciuniv.edu

Abstract

The unique ability to rapidly amplify low copy number DNA has made *in vitro* Polymerase Chain Reaction one of the most fundamental techniques in modern biology. In order to harness this technique to its full potential, certain obstacles such as nonspecific by-products, low yield and complexity of GC rich and long genomic DNA amplification need to be surmounted. As *in vitro* PCR does not have any regulatory mechanisms unlike its counterpart *in vivo* DNA replication machinery, scientists often use a number of additives like glycerol, betaine, dimethyl sulphoxide and formamide in order to achieve the perfection of *in vivo* system. In the last two decades nanotechnology has provided excellent solutions to many classical problems in various scientific fields including biotechnology and recently the PCR technique has begun to benefit from this so called "Nano Era". In this review, impacts of several nanomaterial on PCR efficiency, specificity and fidelity are described in accordance with the recent literature. Putative interaction mechanisms between nanomaterials and primary PCR components are also addressed in a comprehensive manner.

Keywords: Polymerase chain reaction, nanomaterial-assisted PCR, carbon nanotubes, graphene, gold nanoparticles

1. **Introduction**

In vitro Polymerase Chain Reaction (PCR) was first reported by Kjell Kleppe and 1968 Nobel laureate H. Gobind Khorana[1] and further improved by 1993 Nobel laureate Kary Banks Mullis,[2] who described the method as a "Classical Eureka!" moment.[3] Polymerase Chain Reaction, repeated cycles of *in vitro* DNA synthesis, has shortly become a fundamental technique in molecular biology, biotechnology and clinical medicine following the discovery of a thermostable DNA polymerase enzyme.[4] PCR was well-described as: "The process which comprises treating of separate complementary strands of a target nucleic acid with a molar excess of two primers and extending the primers to form complementary primer extension products which in turn act as templates for synthesizing the desired nucleic acid sequence".[5] PCR technique has been used immensely for a wide variety of applications including mutation detection,[6] gene cloning,[7] genotyping,[8] microarray,[9] DNA sequencing,[10] fingerprinting,[11] paternity testing,[12] pathogen detection,[13] forensics[14] and diagnostics.[15]

The significance of PCR originates from its ability to amplify trace amounts of DNA or cDNA (complementary DNA) sequences within minutes in a reaction realized in an automated machine.[16] A successful PCR reaction ideally generates only one amplification product, which is the target sequence with high specificity and fidelity. However, it is well known that PCR is an error-prone reaction due to its *in vitro* nature; therefore specificity, fidelity and efficiency of PCR are not always satisfactory even after laborious optimization efforts. These drawbacks originate from the fact that PCR does not have any replication control mechanism unlike its counterpart *in vivo* DNA replication, which operates exclusive enzymes and proteins for the maximum specificity, such as single stranded DNA binding protein.[17] Subsequently, PCR produces target amplicon accompanied by non-specific side products called PCR artifacts.[18] The main types of PCR artifacts can be categorized as the ones coming from template DNA sequence as a result of chimerical molecule formation and those originating from the skewed template to product ratio due to different amplification or cloning efficiencies.[19–21] There are also DNA sequences which are exceptionally difficult to amplify due to their long and GC-rich nature.[22] As a result of the stated complications, enhancement of PCR becomes imperative to meet and exceed the current challenges in experimental and clinical biology. Optimization of critical parameters in PCR, such as magnesium ion concentration, annealing temperature, cycle number, template quality, type and concentration of DNA polymerase enzyme and incorporation of

various additives, are found to be vital in order to improve the final product sensitivity and efficiency. Several chemical and biological additives including but not limited to glycerol,[23] formamide,[24] betaine,[25] 7-deaza-2'-deoxyguanosine[22] and DMSO[26] have been included in PCR, moreover, new PCR techniques such as hot start PCR[27] and touchdown PCR[28] are developed in order to achieve higher efficiency and specificity in the reaction.

With the emergence of nanotechnology in 1980s,[27] nanomaterials have gained considerable attention from numerous disciplines owing to their exceptional physical and chemical properties like high thermal conductivity and high surface to volume ratios.[28–30] Nanomaterial-assisted PCR, so-called nano PCR,[31] is a new area in biotechnology that introduces nanostructured materials into PCR reaction to obtain improved specificity and yield results. To date, gold nanoparticles (AuNPs),[32] graphene oxide (GO),[33] reduced graphene oxide (rGO),[33] quantum dots (QDs),[34] upconversion nanoparticles (UCNPs),[35] fullerenes (C_{60}),[36] carbon nanotubes (CNTs),[37] some other metallic nanoparticles[38] and nanocomposites[39] have been investigated for their capability in PCR enhancement. In this review, recent progress on nanomaterial-assisted PCR is discussed with an emphasis on its advantages/disadvantages. The potential interaction mechanisms between nanomaterials and PCR components are also discussed comprehensively. This review provides useful insight for mechanism studies and future applications of nanomaterials in PCR.

2. Gold Nanoparticle Assisted Polymerase Chain Reaction

Colloidal AuNPs have been used since ancient times owing to their dynamic colors formed via their special interaction with visible light. Unique properties of AuNPs, such as tunable size and physical dimensions, electronic, optical and catalytic activity, high surface-to-volume ratio, stability, biocompatibility and ease of surface modification have made AuNPs excellent scaffolds for nanobiotechnology. Applications of AuNPs in current medical and biological research includes biodetection,[40] biodiagnostics and biosensors,[41] drug delivery,[42] immunoassay studies,[43] photothermolysis of cells,[44] bioimaging,[45] genomics[46] and PCR enhancement.[47]

The first report of colloidal gold additive in PCR reveals that AuNPs are able to enhance the specificity of PCR product significantly. In order to investigate the phenomenon, Li et al.[47] selected an error-prone PCR system with a 283 bp λDNA as template. In the presence of citrate-stabilized AuNPs at low concentrations

(0.2-0.8 nM), unprecedented yield and specificity enhancement were observed in the PCR amplification. It was also demonstrated that AuNPs induced a substantial yield improvement without any loss in specificity even at significantly low annealing temperatures (25-40 C°). Within the same year Li et al.[48] reported that AuNPs contributed to the final efficiency of Real-Time PCR as well as conventional PCR. In the study, PCR time was shortened without any loss in the yield, and the reaction sensitivity was improved by 5-10 and 10^4 fold in conventional and quick PCR systems, respectively. Furthermore, Yang et al.[49] proposed that specificity and yield improvements in AuNP-assisted PCR could depend on the type of DNA polymerase used in the reactions. It has been stated that the optimized amount of AuNPs could shift threshold cycle (C_T) values of real-time PCR when using increased amounts of wild type *Taq* DNA polymerase, however, no significant change in C_T values was observed for recombinant *Taq* DNA polymerase. In contrast, Haber et al.[50] observed neither efficiency nor specificity enrichment in their AuNP-assisted Real-Time PCR study of three different DNA sequences. As a result of fluorescent quenching of SYBR Green I by AuNPs, the authors indicated the significance of optimization of real time PCR parameters. On the other hand, Vu et al.[51] observed that AuNP-assisted PCR favored shorter sequences rather than longer sequences in their semi-multiplex PCR study. In light of these findings, similar promising applications of AuNP-assisted PCR have been reported for detection of Japanese encephalitis retrovirus,[52] genotyping of long-range haplotypes[46] and amplification of GC-rich DNA templates.[53]

Despite substantial research on AuNP assisted PCR the fundamental interaction mechanism of AuNPs within PCR system has not been entirely clarified yet. Initially it has been proposed that AuNPs act in a way similar to single-stranded DNA binding protein, which plays a vital role in the specificity of *in vivo* DNA replication machinery[47] and improve overall heat circulation in PCR solution.[48] The latter has been discarded since the optimized concentration of AuNPs was significantly below the reported values which could induce a substantial increase in thermal conductivity.[54,55,50,51] Furthermore, it has also been found that excess amount of AuNPs totally inhibit the PCR reaction[47] and remarkably, inhibition assays revealed the fact that total surface area of AuNPs was governing the inhibition mechanism rather than the particle size.[56,51] Inhibition effect of AuNPs is shown to be reversible in the presence of higher concentrations of DNA polymerase or other proteins like BSA and Thrombin, where both proteins compete with DNA polymerase in order to bind on AuNP surface due to Vroman-like effect.[57,58]

DNA polymerase enzymes have potential to strongly adsorb on AuNP surface via polar groups in their amino acid structure. Although entire side groups of the protein are not positively charged to assure a complete interaction with the negatively charged citrate-capped AuNPs, the collective binding of functional groups would eventually favor a certain level of adsorption. Since there is no evidence for irreversible adsorption mechanism, the adsorption-desorption kinetics on AuNPs would determine the activity of DNA polymerase within PCR. One would think that AuNPs might decrease the efficiency of PCR due to lowered enzymatic activity, however, interaction of other PCR components with AuNPs could still enable the amplification of PCR product.[59] Mi et al.[60] reported that AuNPs prevents the activity of *Pfu* DNA polymerase at low temperatures similar to the effect of Mg^{2+} in a conventional hot-start PCR, thus, stimulating one pot hot-start effect in routine PCR as shown in **Figure 1**. In the same study, Mi et al. also demonstrated that *Pfu* and AuNP-modulated *Pfu* gave error rates of 1.16×10^{-6} and 1.10×10^{-6}, respectively, which were close to the reported value of 1.30×10^{-6} for *Pfu*, obtained from a PCR-based forward mutation assay utilizing the well-characterized *lacI* target gene. In consistent with this result, the error rates of 5 nm AuNP, 10 nm AuNP assisted PCR and the control PCR were found to be 7.28×10^{-6}, 26.62×10^{-6} and 5.26×10^{-6}, respectively.[61] Interaction between *Pfu* DNA polymerase and AuNPs could be strong enough to reduce overall activity of *Pfu* DNA polymerase at the annealing step. Consequently, AuNPs can hinder the non-specific amplification by avoiding unsolicited mispriming and primer-dimer formation. Similarly, Mandal et al.[62] showed that the denaturation point of *Taq* DNA polymerase enzyme increased from 73 to 81 $^\circ$C in the presence of AuNPs, which has resulted in enhanced PCR yield. This enhancement mechanism could be explained by the increase in active enzyme concentration at extension step of PCR.
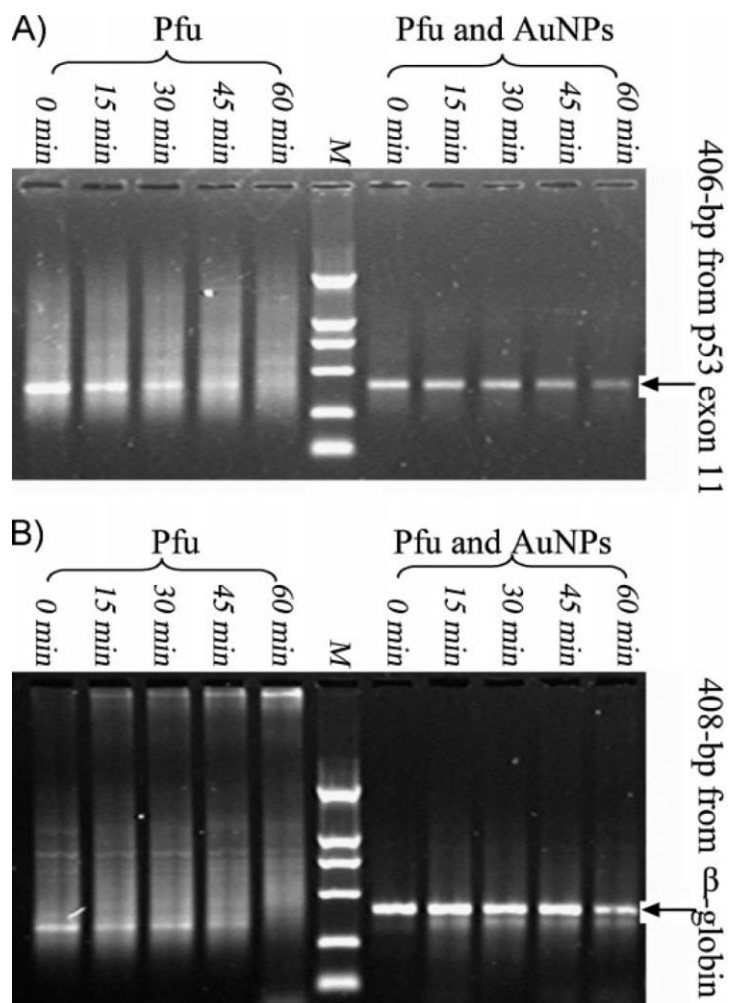
Figure 1: PCR amplification performance of *Pfu* (left five lanes) and nano-engineered *Pfu* (right five lanes) for p53 exon 11 gene (406 bp) and β-globin gene (408bp). Time scale indicates the incubation of *Pfu* and *Pfu*-AuNP complex at 58 °C, M represents molecular weight marker. Reproduced with permission from ref.[60] Copyright © 2009 Wiley-VCH Verlag GmbH & Co. KGaA, Weinheim.

Whilst the following studies focused on the theory that AuNPs mostly interact with DNA polymerase and modulate its conformation and function under certain conditions;[62,59,60] Vu et al.[51] reported that Hexadecanethiol-coated AuNPs did not affect PCR specificity or efficiency, which revealed the fact that examination of surface properties, is also essential to comprehend AuNP-assisted PCR mechanism.

6

- Hydrophilic, negatively charged phosphate backbone of DNA (PO_4^-) repels negatively charged AuNPs, thus the backbone is mostly exposed to solution

- Positively charged groups in nucleotides (NH_2) face to the AuNP surface, which forms an electrical double layer

- As a result, ssDNA (primers, short DNA templates) reversibly adsorbs on the AuNP's surface via electrostatic interactions

- Desorption of the attached molecules occur in the presence of complementary sequences, which prevent mis-pairing or primer dimer formation resulting in enhanced PCR specificity
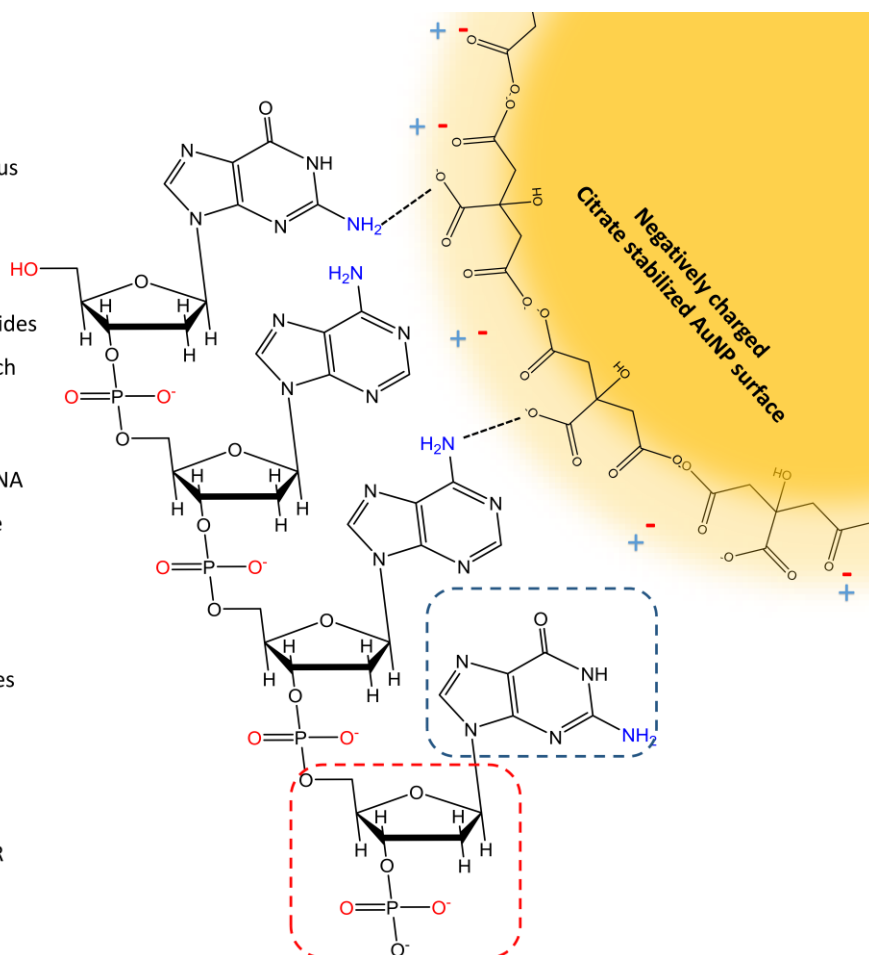
Figure 2: Possible formation of electrical double layer around AuNPs upon binding to single-stranded DNA

Together with DNA polymerase effect, probing the interaction between AuNPs and other PCR components (primers, templates) is essential to understand the AuNP assisted PCR mechanism in detail. On account of their short, single-stranded structures, primers or short DNA templates tend to bind on AuNPs by positioning their negatively-charged phosphate backbone away from negatively-charged citrate-capped AuNPs surface, which forms a dielectric double-layer[63,32,64] as presented in **Figure 2**. Similar to DNA polymerase-AuNP interaction, DNA-AuNP interaction is also based on adsorption-desorption kinetics. Since the size of primers is smaller than DNA polymerase, their kinetics are not severely restricted at bio-nano interface, however, reactivity of primers is constricted at low temperatures. In this perspective, AuNPs could be generating a useful constraint on primer kinetics by decreasing the active primer concentration at low temperatures, which reduces self-primer interactions during annealing step. It is well-established that once short ssDNA sequences attach on the surface of AuNPs, they display a strong propensity to stay on the AuNP surface unless they interact with a complementary sequence.[65,63] This could explain the improved specificity and

yield in AuNP-assisted PCR for short templates, in which DNA templates on the gold surface only interact with primers or their complementary sequences, which eventually prevent heteroduplex formation. Examples presented in **Table 1** suggest that template DNA sequence, primers, type of DNA polymerase enzyme as well as size and surface modification of AuNPs are all critical for the PCR enhancement. Thus, it is imperative to evaluate all these factors on a case-by-case basis.

Table 1: Effects of AuNPs on Polymerase Chain Reaction

AuNPs	Size (nm)	Conc. (nM)	Impact	DNA (bp)	Enzyme	Mg (mM)	Ref.
Citrate-Stabilized	10	0.4	Improved specificity and efficiency	λ-DNA (283 bp)	Ex *Taq*	-	[47]
Citrate-Stabilized	13	0.7	Improved efficiency	EGFP-I (173 bp), PT4K2B (752 bp), MS1R (1236 bp), BNIP3 (238 bp)	Supertherm *Taq*, YEA *Taq*	-	[48]
Citrate-Stabilized	12±2	0.2-1.6	No effect	fatA (76 bp), RT73 (108 bp), RT3 (273 bp)	Taqman Probe	-	[50]
Citrate-Stabilized	13.2±2.4	1.6	Improved specificity and efficiency	JEV E gene	*Taq*	2×10^{-6}	[52]
Citrate-Stabilized	10	0.4	Improved specificity and efficiency	λ-DNA (283 bp), DENV-4	Go*Taq*	-	[51]
Citrate-Stabilized	10	2.09	Improved efficiency	λ-DNA (792 bp)	*Taq*	3	[49]
Citrate-Stabilized	10	0.38	No Effect	λ-DNA (792 bp)	rTaq	3	[49]
Citrate-Stabilized	5	1.36	Improved specificity and efficiency	pBR322/Pst I (309 bp), p53 exon 11 (406 bp), β-globin (408 bp)	*Pfu*	0.08	[60]
Citrate-Stabilized	5, 10, 20	13, 2.85, 0.63	Inhibition	Salmonella enterica ATTC 13311 (119 bp)	iTaq	3.5	[56]
Citrate-Stabilized	5	1.36	Improved specificity and efficiency	SNP loci	*Taq*, LA *Taq*	3.5	[46]

Citrate-Stabilized	13	1.36	No Effect	pM18-T (309 bp)	*Pfu*	-	[59]
G5.NH$_2$-modified	1.9-2.6	0.37-0.51	Improved specificity and efficiency	λ-DNA (283 bp)	Ex *Taq*	1.5	[66]
Citrate-Stabilized	13	0.05	Improved specificity and efficiency	GEN, HBV	*Taq*	1.5	[32]
Citrate-Stabilized	11	2	Improved efficiency	GAPDH	*Taq*	1.5	[62]
Citrate-Stabilized	10	0.5, 2.28	Improved specificity and efficiency	GNAS1	*Pfu*, r*Pfu*	-	[53]
Citrate-Stabilized	10	0.35, 1.14-10	Improved specificity and efficiency	GNAS1	*Taq*, Ex *Taq*	-	[53]
PDDA-modified	1.9-2.6	1.54x10^3	Improved specificity and efficiency	λ-DNA (283 bp)	*Taq*	1.5	[67]

Utilization of AuNPs in PCR has shown significant specificity and efficiency improvement in a number of studies. There are few points to emphasize in order to summarize the overall interactions of AuNPs with the major PCR components; a) AuNPs enable the use of low annealing temperatures during PCR, which reduces the optimization step b) AuNPs provide adsorption surfaces for primers and short DNA templates, which help preventing mispriming and primer dimer formation, c) the denaturation temperature of the DNA polymerase increases in the presence of AuNPs which contributes to the number of active enzymes operating at the extension step of PCR, d) effect of AuNPs can differ from one assay to another as a result of different binding affinities of nucleobases towards AuNPs. For example, adenine has higher affinity for Au surfaces than thymine. On the other hand, Guanine and Cytosine show similar but moderate affinities to Au surfaces.[68] Consequently, AuNP-biomolecule interactions should be investigated further by giving attention to the size, surface charge and concentration of the nanoparticle, which could be useful to reveal the specific conformational changes of the adsorbed molecules which might prevent their activity.

3. Carbon Nanotube Assisted Polymerase Chain Reaction

Carbon nanotubes are allotropes of carbon with a cylindrical shape of sp^2-hybridized carbon atoms.[69] The name CNT is derived from its long, hollow structure with the walls formed by single atom-thick sheets of carbon, called graphene.[29] CNTs are constructed with a length-to-diameter ratio of up to 132,000,000:1, which is greater than any other standard material.[70] Depending on their size in diameter, CNTs are categorized as single-walled carbon nanotubes (SWCNTs; 0.4–2 nm) and multi-walled carbon nanotubes (MWCNTs; 2–100 nm).[71] Characteristic properties of CNTs such as high electrical and thermal conductivity, high aspect ratios, exceptional mechanical strength and rigidity have given rise to their use in a variety of applications including electrochemical energy storage and production,[72] field emission,[73] biosensor construction,[74] atomic force microscopy,[75] imaging[76] and DNA nanotechnology.[77] Among these, the discovery of DNA-assisted dispersion and separation of CNTs has opened up new avenues for CNT–based biotechnology research,[78,79] one of which is addition of carbon nanotubes into biochemical reactions like PCR.

First utilization of CNT in PCR has been reported by Cui et al.[80] where SWCNTs are promoted as PCR enhancers. According to the findings, the final yield of PCR product increased with the addition of SWCNTs up to 3 µg/ml, however, the reaction was completely inhibited with increasing concentrations. Noticeably, the authors obtained similar results without including Mg^{2+} in the reaction, which is an essential cofactor for DNA polymerase enzyme to maintain its activity. Although High Resolution Transmission Electron Microscopy (HRTEM) and X-Ray Photoelectron Spectroscopy (XPS) data implied a potential physical interaction between SWCNTs and PCR components, the underlying reason of such interaction might be merely the solvent evaporation effect. Since water has a considerable amount of surface tension energy, the liquid–gas interface can carry particles into a limited space during its evaporation. Eventually, free components of sample would tend to concentrate on the first surface available.[81,82] Therefore, interactions at bio-nano interface should be further investigated by the techniques that allow to assess materials in their native environment, such as Circular Dichroism (CD) spectroscopy, In situ Atomic Force Microscopy (AFM) and Nuclear Magnetic Resonance Spectroscopy (NMR).

In another study conducted by Zhang et al.[83] improved PCR efficiency and specificity by incorporation of CNTs has been reported where a long 14.3kb lambda DNA was used as template. After performing PCR containing different types of carbon-based nanomaterials (carbon nanopowder, SWCNTs and MWCNTs

with different size and surface properties) at various concentrations (max 1 mg/ml) it is found that all the tested nanomaterials increased the efficiency and specificity of PCR with a CNT concentration of approximately 0.8 mg/ml. To assess the fidelity of the CNT-assisted PCR, Zhang et al.[83] evaluated Sanger sequencing data of CNT-free PCR and CNT-assisted PCR (SWCNT and MWCNT). The preliminary results showed no significant drop in DNA replication fidelity in comparison to the conventional PCR. Additionally, Shen et al.[61] found the error rates of control PCR, SWCNT and MWCNT assisted PCR as 5.26×10^{-6}, 16.25×10^{-6} and 32×10^{-6}, respectively, which was better than the error rate of betaine (69×10^{-6}). Despite the fact that the current fidelity results are not sufficient enough to prove CNT as a viable PCR additive, the data is still promising for further investigation of CNTs in PCR.

There are a large number of reports proving the exceptional thermal[84] and mechanical[85] properties of CNTs, however, there is still lack of information on the impact of these parameters in PCR which is already a heat-transfer technique. It has been reported that thermal conductivity of individual SWCNTs (9.8 nm in diameter) measured at room temperature surpasses 2000 W/mK and increases as its size decreases in diameter.[86] Although the thermal conductivity of bulk CNTs is lower than SWCNTs, the minimum thermal conductivity is still significantly higher than pure water (0.6 W/mK at 20 °C).[87] This information proposes that CNT-containing PCR suspension would have a higher thermal conductivity and thus could provide a better thermal transfer and heat equilibrium in PCR tubes. Based on this assumption, Quaglio et al.[88] introduced metallic MWCNTs into Poly (Dimethyl) Siloxane (PDMS/CNTs) to monitor alteration in PCR efficiency originating from only thermal properties of the nanocomposite. In the experiment, nanocomposite is deposited on a chip based PCR system and blocking the surface with Bovine Serum Albumin (BSA) prevented surface effect of CNTs. The results displayed a considerable reduction in total reaction time by 75% demonstrating the direct advantage of the MWCNTs in the nanocomposite. Consistent with that result, Cao et al.[89] obtained improved PCR products at varying annealing temperatures between 30-55 °C, in which improvement has also been affected by different surface charges of polyethyleneimine-modified MWCNTs. As presented in **Figure 3**, both negatively-charged MWCNTs (acid-treated pristine MWCNTs and succinic anhydride-modified CNT/PEI) and positively charged MWCNTs (CNT/PEI) improved the efficiency and specificity of PCR with optimum concentrations of 2.3×10^{-2} and 6.3×10^{-1} mg/ml, respectively. Nevertheless, neutral MWCNTs (acetic anhydride modified-CNT/PEI) showed neither improvement nor inhibition under

similar conditions. These observations suggest that the mechanism of CNT-assisted PCR cannot be thoroughly explained with improved heat conductivity since other factors such as surface charge and electrostatic interactions between nanomaterial and PCR components also contribute to PCR enhancement. In order to probe the physical interaction between MWCNTs and PCR reagents, major PCR components; primers, template (283bp) and DNA polymerase (recombinant) are individually incubated with negatively-charged acid-treated pristine MWCNT at a concentration of 12.4 mg/ml and then combined with remaining PCR reagents prior to thermal cycling.[89] It has been discovered that incubation of primers and DNA polymerase with MWCNTs prior to thermal cycling decreases the efficiency of PCR slightly as a result of restricted interaction of the template with primers and the enzyme. It should be noted that the type of polymerases (recombinant, mutant, *Taq*, *Pfu* polymerase), primers, length and sequence of templates and physical properties of CNTs vary from one study to another, so owing to their unique structures they might exhibit different behaviors when they are interacted with CNTs. For instance, in contradiction to previous findings, Yi et al.[90] reported that CNTs (SWCNT, SWCNT-COOH, MWCNT and MWCNT-COOH) either reduced or inhibited the PCR reactions where the inhibitory effect increased in the order of CNT-COOH > Pristine CNT and SWCNT > MWCNT. In order to discover the source of inhibition, authors surveyed the interaction between CNTs and wild type *Taq* DNA polymerase by incubating the enzyme with different types of CNTs at various thermal conditions. The data obtained revealed the adsorption of *Taq* DNA polymerase onto the CNTs regardless of their surface charges or functional groups. Interestingly, it has been also stated that the adsorbed enzyme maintained its activity during PCR, which was evident with target bands on agarose gel. In agreement with this result, Williams et al.[37] reported that the adsorption of *Taq* DNA polymerase on SWCNT is unlikely to inhibit PCR reaction. Eventually, inhibition of the reaction is anticipated as nanomaterial-induced formation of free radicals. There is however no direct experimental evidence of oxidative stress caused by CNT-derived free radicals,[91] on the contrary, MWCNTs are shown to have a significant radical scavenging capacity.[92] From a different point of view, if the enzyme were still active after adsorption, the reduced band intensities of the targets would be explained with the adsorption of amplified DNA onto CNTs, which would gradually prevent their visibility on the gel at increasing concentrations. To prove such an adsorption of the amplified DNA, purified PCR products could be subjected to thermal cycle with CNTs at different concentrations and evaluated on a high-resolution gel (for example native polyacrylamide gel) under similar conditions. Additionally, the presence of large CNT

bundles and the formation of the new bundles during thermal cycles could be other reasons for such inhibition, which may be eliminated or reduced by advanced probe-sonication and filtration steps.
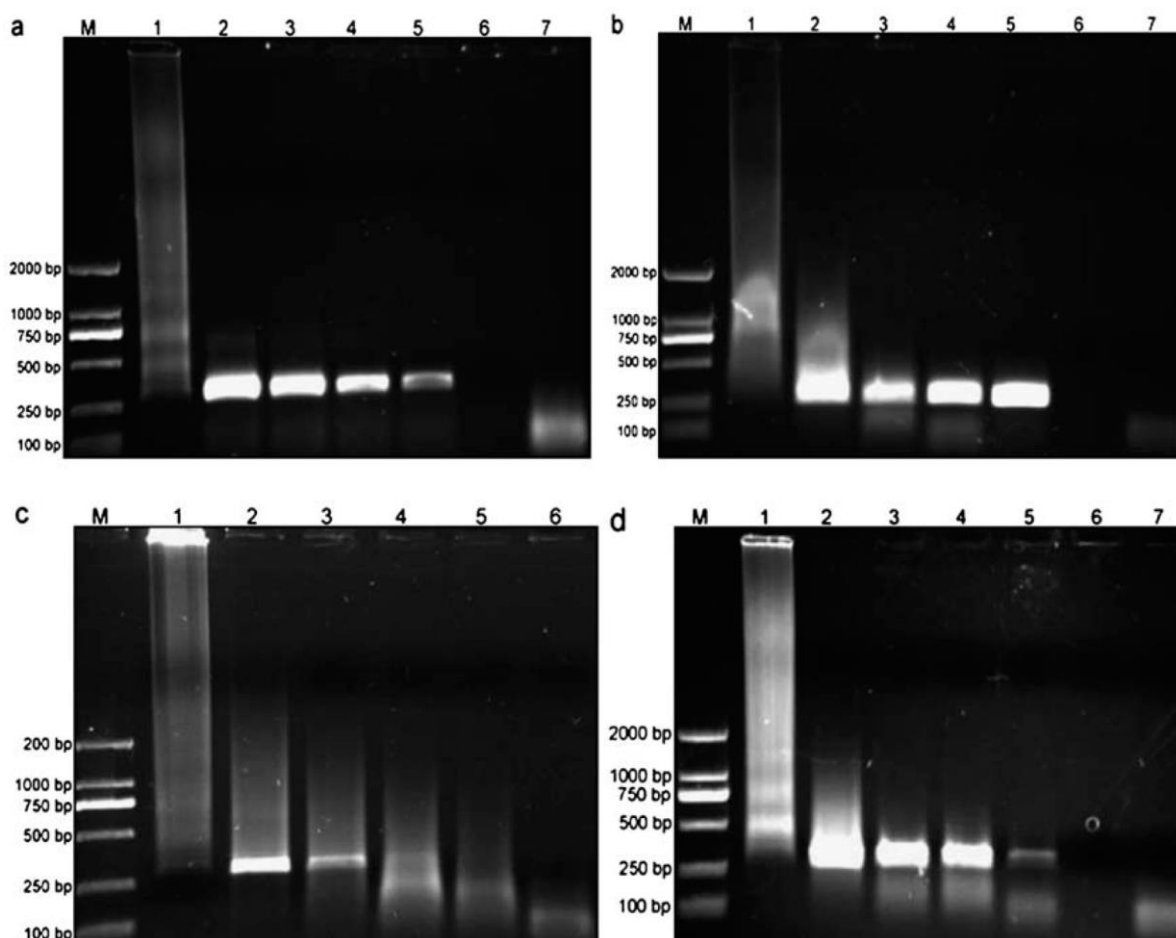

Figure 3: The effect of different surface charges on CNT-assisted PCR. First lane is marker and last lane is negative control **a)** Negatively charged acid-treated pristine MWCNT, from lane 1 to 6, the final concentrations are 0, 15.52, 23.28, 31.04, 38.80, and 46.56 mg/L, **b)** Positively charged PEI-modified MWCNT, from lane 1 to 6, the final concentrations are 0, 0.17, 0.22, 0.28, 0.39, and 0.44 mg/L, **c)** Neutral CNT/PEI modified with acetic anhydride, from lane 1 to 5, the final concentrations are 0, 6.19, 18.57, 30.95, and 43.34 mg/L, **d)** Negatively charged CNT/PEI modified with succinic anhydride, from lane 1 to 6, the final concentrations are 0, 0.54, 0.63, 0.78, 0.82, and 0.86 g/L, respectively. Reproduced with permission from Ref: [89] Copyright © 2009 Wiley-VCH Verlag GmbH & Co. KGaA, Weinheim.

Table 2: Effects of CNT's on Polymerase Chain Reaction

CNT	Size (nm)	CNT (mg/ml)	Impact	DNA (bp)	Enzyme	Mg (mM)	Ref.
SWCNT	2	<3	Increased efficiency	410	*Taq*	0-1.5	[80]
SWCNT SWCNT-COOH MWCNT MWCNT-COOH	<2 10-20	0.05-0.8	Either reduced Efficiency or reaction inhibition	200	*Taq*	3	[90]
SWCNTs MWCNTs CNT-OH CNT-COOH	1-2 <8	0.6-1.2 0.8-1.6	Increased efficiency and specificity, unaffected fidelity	14000	*Pfu, Taq*	2.8	[83]
Negatively charged, pristine, acid-treated MWCNTs	30-70	2.3×10^{-2}	Increased efficiency and specificity	283	*Taq*	1.5	[89]
Positively charged Polyethyleneimine MWCNTs (CNT/PEI)	30-70	3.9×10^{-4}	Increased efficiency and specificity	283	*Taq*	1.5	[89]
Negatively charged Succinic anhydride CNT/PEI	30-70	6.3×10^{-1}	Increased efficiency and specificity	283	*Taq*	1.5	[89]
Neutral Acetic acid anhydride CNT/PEI	30-70	-	Slightly increased efficiency	283	*Taq*	1.5	[89]
Pristine PEI	-	4×10^{-5}	Increased efficiency and specificity	396	*Taq*	1.5	[39]
PDMS/MWCNTs based PCR system	20-70	-	Thermal conductivity induced reaction time improvement	150 756	*Taq*	0.25	[88]
CoMoCAT SWCNT (6,5)	0.8	0.01-1	Slightly increased efficiency	76	*Taq*	-	[37]

As summarized in **Table 2**, most of the reports indicate a concentration and surface charge dependent PCR enhancement via CNTs, regardless of DNA template length. The optimum CNT concentration for PCR enhancement could be suggested below 1mg/ml for most of the applications. However, it should be noted that the concentration of the bundled CNTs and CNT aggregates cannot be measured with solution based UV-Visible Spectroscopy since they tend to precipitate immediately.[93,94] Therefore, the utmost caution

should be taken while sonicating the CNT solutions, especially the pristine CNT solutions due to their hydrophobic nature, in order to eliminate big aggregates and the bundles as much as possible. The exceptional experimental data should be also taken into consideration in order to understand the origin of such inhibition, which is important for further CNT-based biological applications like nanotoxicology. For example, a set of reference carbon nanomaterials would be useful to test their influence in PCR, wherein sequence dependency could be investigated by using a randomized oligonucleotide library, likewise, enzyme dependency could be tested by employing a number of different polymerase under equal conditions. Another research on the effect of zeta potentials of CNTs in PCR could be useful to identify the exact functions of surface polarities. Finally, a particular research on the effect of CNT length in DNA amplification should very useful to evaluate the aggregation states of the CNTs during PCR, which could enlighten the roles of well-dispersed individual tubes, bundles or aggregates in PCR.

4. Graphene Oxide and Reduced Graphene Oxide Assisted Polymerase Chain Reaction

Graphene oxide (GO) is a unique 2D carbon material which exhibits graphene like properties and can be readily dispersed in water and other organic solvents unlike pristine graphene. GO is obtained from exfoliation of graphite oxide which is produced via well-known Hummers method.[95] Treatment of graphite oxide with strong oxidizing agents like sulfuric and nitric acid can decorate graphite flakes with hydroxyl, carboxylic acid and other oxygen rich functional groups. Subsequent high frequency sonication of graphite oxide results in a few layer thick hydrophilic GO flakes. Ease of functionalization,[96] unique optical[97] and mechanical properties,[98] excellent fluorescence quenching ability[99] and hydrophilic nature have enabled GO to be used in various biomedical research applications including PCR.[100] On the other hand, GO can be transformed into reduced GO (rGO) by using chemical, thermal and electrochemical techniques in which rGO regains considerable amount of sp^2-hybridized carbon network structure and semi-metal properties due to the improvement in sheet resistance of several orders of magnitude.[101] In addition, removal of oxygen-rich functional groups from the surface, while protecting the side functional groups, retains its solubility to certain extent. Like GO, rGO has also been utilized in a wide range of biological applications.[102]

Employment of GO in PCR has first been reported by Jia et al.[33] who revealed that specific concentrations of GO provided a single specific band of desired product without any artifacts. While concentrations less than 12 μg/ml didn't show any improvement in terms of specificity enhancement, the concentrations above 70

µg/ml inhibited the PCR reaction completely. The authors stated that the GO concentration in the range of 12-60 µg/ml was optimum for enhanced PCR specificity. Interestingly, GO did not show enhancement of the specificity of repeated PCR unlike rGO which enhanced the specificity till 8th round in spite of some non-specific bands accumulated from the previous cycles as presented in **Figure 4**. This phenomenon has been attributed to strong electrostatic repulsion between DNA molecules and negatively charged GO compared to the electrostatic repulsion between DNA molecules and rGO, which has less surface negative charge compared to GO. This has been proved by X-ray photoelectron spectroscopy and FTIR. In addition, a π-π stacking between the ring structures of nucleotides and hexagonal cells of rGO has also been revealed.
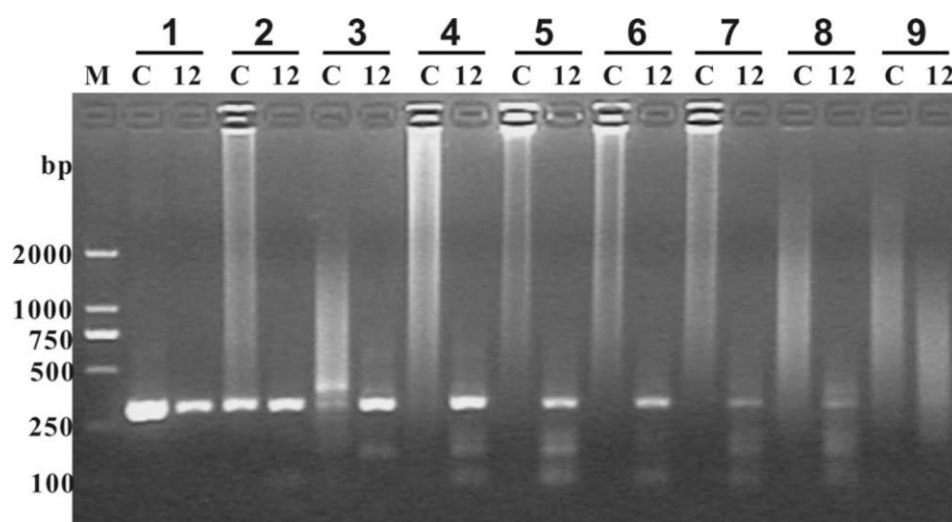

Figure 4: The effect of rGO in nine rounds of error-prone PCR. The template is a pET-32a plasmid DNA of 300 bp; **M:** DNA marker; **C:** No rGO in reaction; **12:** rGO concentration in µg/mL. Reproduced with permission from ref: [33] Copyright © 2012 Wiley-VCH Verlag GmbH & Co. KGaA, Weinheim.

Alternatively, rGO has been tested in another error-prone PCR system with a different template and same effect has been observed with 8 µg/ml as an optimal concentration whilst 12 µg/ml was found to inhibit the process completely. Similar concentration dependent PCR enhancement studies have also been carried out by Khaliq et al.[103] using graphene nanoflakes.

As stated in earlier sections, annealing temperature is an important factor for reliable PCR amplification. In conventional PCR, the annealing temperature is usually chosen between 45-65 °C.[104] Using rGO, highly specific target bands were obtained at temperatures as low as 25 °C and further increasing the annealing temperature did not affect the product specificity.[33] Even though experimental results showed that both GO and rGO improve the specificity of PCR, rGO provides multiple-round PCR enhancement at lower

concentrations in comparison to GO. Combining all the available information about GO/rGO-assisted PCR and some other associated information from the recent literature, it could be possible to interpret the interaction of graphene and derivatives with PCR components as summarized below:

- **Interaction with DNA on the large surface area:** Since overall negative charge distribution on the surface of GO is significantly higher than rGO, negatively charged phosphate backbone of dsDNA would experience a higher electrostatic repulsion from GO surface compared to rGO surface. On the other hand, ssDNA which has one unpaired phosphate backbone would easily bind on GO surface due to non-specific hydrogen bonding[105] as illustrated in **Figure 5**. Due to the surface functional groups, GO may induce a kinetic barrier for ssDNA to be released back into the reaction. Unlike GO, rGO contains relatively high sp^2-hybridized carbon network, less oxygen containing functional groups and nitrogen containing positively charged functional groups. Since the stimulated kinetic barrier is lower in the case of rGO, rGO may offer more convenient platform for the amplification.

- **rGO-DNA polymerase interaction via surface charges:** rGO, which is negatively charged, forms a positively charged complex by interacting with DNA polymerase. Addition of DNA polymerase to rGO solution changes the zeta potential of rGO forming a much DNA-friendly environment. Jia et al.[33] confirmed this phenomenon by further adding BSA in different concentrations to the PCR system which also proves that rGO has a strong interaction with DNA polymerase. Higher concentrations of BSA resulted in non-specific bands, which may be due to the severed interactions between rGO and DNA polymerase.
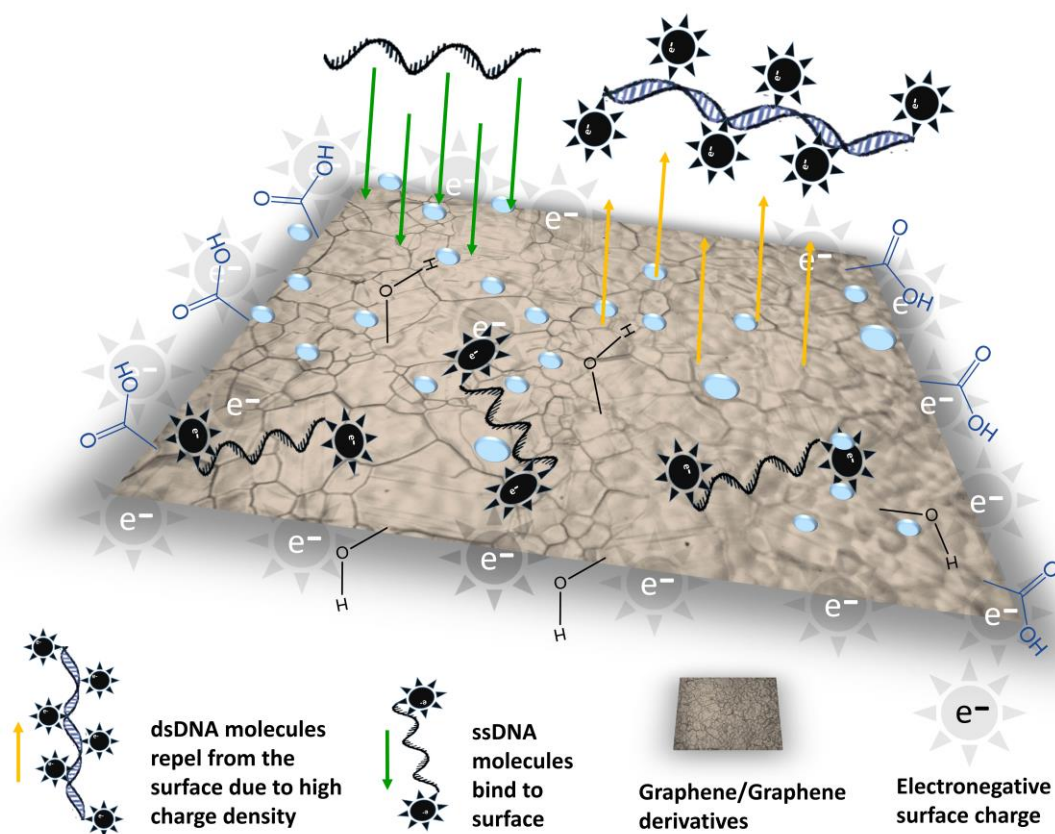
Figure 5: Interaction of ssDNA and dsDNA with graphene derivatives

- **Effect of high thermal conductivity:** PCR specificity enhancement is also attributed to heat transfer properties of the nano additives.[48] The higher the thermal conductivity of the material, the better is the specificity.[103] Balandin et al.[106] have experimentally obtained the thermal conductivity of graphene as 5300 W/mK at room temperature. This extremely high value outperforms all the existing conventional materials which are used and tried for PCR specificity enhancement.

Even though the review is related to the PCR specificity enhancement using nanomaterials, the authors would also like to give an insight in to the direct and indirect effects of using nanomaterials with biomolecules. Our literature study states that nanomaterials enhance PCR efficiency and specificity; nevertheless it is a possibility that these nanomaterials may affect the downstream use of these PCR products. Recently, Liu et al.[107] have shown that GO can induce mutagenesis in both *in vivo* and *in vitro*. This states that though there is a reduction in non-specific bands through nanomaterial-assisted PCR, the collected data may not be entirely reliable at cellular level. Further studies are needed in this aspect to find

the right combination of parameters. One such study the authors would like to suggest is that using a nanomaterial coated/integrated PCR tube rather than mixing the nanomaterial with reagents. This approach could avoid the direct chemical interaction of biomolecules with the nanomaterial and at the same time enhance the PCR specificity as a matter of surface property. This process also can remedy the issue of PCR product separation from nanomaterial suspension. To support this method we would like to cite few examples from the literature on the toxicity of GO and rGO to living cells.[108] According to Liu et al.[107] GO sheets wrap individual cells from the solution unlike rGO where the cells are trapped. The studies have shown that cell trapping by GO is more non-viable to cells compared to cell trapping by rGO. In cell wrapping the surface of the cells is in direct contact with GO sheets causing membrane stress, which is affecting the chemical mechanisms within the cell. Similarly, the bacterial cell membrane could be damaged by sharp edges of GO flakes upon direct contact.[109] On the other hand, studies also show that GO substrates accelerate stem cell differentiation.[110] In this aspect the substrates (glass/silicon/silicon dioxide) has been coated with GO and the cells were placed on top of that unlike the above mentioned methods where GO flakes were suspended along with cells in a solution. To conclude, the authors would like to propose using GO/rGO coated PCR tubes rather than suspending GO/rGO along with individual PCR components. Theoretical studies so far form a base for this method though further work has to be carried out in integrating GO/rGO efficiently within the PCR tubes.

5. Quantum Dot Assisted Polymerase Chain Reaction

Quantum dots (QDs) are semiconductor nanoparticles with dimensions in the range of few nanometers to few microns. Their optical and electrical properties, emerging from the quantum confinement can be tuned by their size and shape. QDs have numerous biological applications in gene technology,[111] whole body imaging,[112] tumor targeting,[113] pathogen and toxicity detection[114] and enhancement of PCR.[115] The current part of the review focuses on PCR enhancement studies using QDs.

Wang et al.[116] reported the first use of QDs for PCR specificity enhancement at different annealing temperatures and different template DNAs. Comparative PCR amplification studies using AuNPs and CdTe QDs suggest that both show similar amplifications except that QDs requires higher concentrations than AuNPs.[48,117] Similar to other nanomaterials, QDs increase the specificity up to certain optimum

concentrations as higher concentrations inhibit the amplification process. Xun et al.[118] reported that the thermal cycling durability and PCR compatibility of QDs can be extended by treating them with PEG 2000. This treatment helps the QDs to extend their fluorescence stability without precipitating during PCR.

Different studies suggested different optimal concentrations of QDs for enhanced PCR, though these concentrations are independent of type of PCR, template length and emission wavelengths. Using QDs, PCR specificity enhancement has been mainly observed with small to medium length DNA fragments rather than longer fragments.[116] An interesting phenomenon suggested by Liang et al.[115] are the optimization of the PCR process by QDs itself and the authors attributed this phenomenon to the affinity between DNA polymerase and QDs. A similar study which explains the affinity between the QDs and DNA polymerase has been reported by Sang et al.[117] In annealing temperature studies using QDs, specific target bands are obtained at temperatures as low as 30 $^{\circ}$C[116] similar to GO and AuNP assisted PCR studies.

Another interesting study would be to know whether the PCR specificity enhancement is due to the surface properties of the QDs or QDs itself. Lu ma and coworkers[34] published the results in which they suggested that the PCR specificity enhancement was due to the QD itself rather than the surface property, which can be altered. In spite of a number of reports on PCR enhancement ability of QDs which is summarized in **Table 3**. On the other hand, only Sang et al.[119] reported a study on the fidelity of QD-assisted quantitative PCR by using Rpsl-based fidelity assay, which is good for measurement for low frequency mutations. According to the results, QDs only slightly introduced more mutations than the blank control, but lower than a frequently used PCR enhancer, betaine. Thus the results were found good enough for most short-length quantitative PCR experiments

Table 3: Effect of different QDs on Polymerase Chain Reaction

QDs	Size (nm)	QD [nM]	Effect	Target (bp)	Enzyme	Annealing (^{0}C)	Ref.
Carboxyl based QDs	2-10	4	Increased specificity	297/530	*Taq* DNA polymerase	30-45	116
CdTe QDs	4.5	60	Increased specificity	310	*Taq* DNA polymerase	55	115
CdSe QDs (MAA coated)	4.1/ 2.5	30	Increased yield & specificity	120	*Taq* DNA polymerase	25-45	34

CdSe/ZnS QDs	22	30	Thermal cycling durability & PCR compatibility	300/245/400	Ex *Taq* DNA polymerase	60	[118]
CdTe QDs	-	85	Increased yield and decent fidelity in qPCR	120/900	*Taq* DNA polymerase	56	[119]

The previous studies related to QD-assisted PCR suggest that QDs cannot increase the efficiency of PCR,[115,116] because, theoretically QDs are semi-conductors unlike AuNPs or graphene which are highly conductive, indicating low thermal conductivity. Recently, Sang et al.[120] reported that using CdTe QDs the PCR reaction time could be significantly shortened without compromising the efficiency in the PCR which can be considered as an important step in QD-assisted PCR research.

Like other PCR enhancing nanomaterials QDs also increase the specificity of the amplification process. The reason for the specificity enhancement is similar to that described for rGO where the modified surface of the QDs is negatively charged because of the carboxyl groups. Due to electrostatic repulsion, negatively charged dsDNA (with high charge density) tend to repel from QDs[121,63] unlike ssDNA which has a lower charge density resulting in QDs binding to ssDNA. Interaction of BSA with QDs has also been confirmed by many researchers which can cause reverse effects on PCR.[115,118] Though there hasn't been any direct evidence of the side effects on the QD assisted PCR product, it might be a possibility as long as the QDs are not completely recovered from the PCR product before further analysis.

6. Impacts of Other Nanomaterials in Polymerase Chain Reaction

Nanomaterial assisted PCR studies are not limited to the above-mentioned nanomaterials. In fact, impacts of several other nanomaterials like metal oxide nanoparticles, noble metal nanoparticles and polymeric nanoparticles have also been studied in parallel as summarized in **Table 4**.

The utilization of C_{60} in PCR has been first reported by Liang et al.[36] where water insoluble C_{60} has been dispersed with the help of Poly (vinyl-pyrrolidone) as a biocompatible surfactant. While a significant decrease in the melting temperature of DNA template along with a dramatic improvement in the qPCR efficiency (in the beginning of exponential phase at lower C_T values) has been observed upon addition of C_{60}, an inhibition took place at later stages, which was attributed to reduce enzymatic activity. Further experiments and simulation studies with water-soluble C_{60} derivatives shed a light on the interaction of DNA

21

polymerase with C_{60} molecules. Shang and coworkers[122] reported that 0.4 μM concentration of $C_{60}(OH)_{20}$ fullerene derivative completely inhibited the activity of *Taq* polymerase in PCR reaction. Atomistic molecular dynamic (MD) simulations exhibited a clear inclination for hydrogen bonding between $C_{60}(OH)_{20}$ molecules and PCR components. In a later study, Govindan et al.[123] proposed the inhibition route of *Taq* polymerase upon interaction with fullerene derivatives, fullerenol and fullerene trimalonic acid. Considering molecular docking and MD simulation results, fullerene derivatives lead a conformational change on *Taq* polymerase originating from close dynamical contact between thumb and finger domains of the protein. Consequently, new configuration of the enzyme severely affected the proficiency of *Taq* polymerase to capture DNA.

Titanium dioxide (TiO_2) nanoparticles and Zinc oxide (ZnO) nanostructures have also been investigated in PCR studies due to their unique surface chemistry. Khaliq et al.[38] reported seven-fold improvement in the PCR efficiency using TiO_2 nanoparticles. Optimized concentration of TiO_2 (0.4 nM) has been used to amplify different sizes of DNA templates with 46-66 % GC content, in which the yield was improved by 2.9-6.9 fold and reaction time was shortened by 50%. Similarly, Xu et al.[124] reported optimized concentration of TiO_2 as 0.6 nM in their PCR detection of bacterial aerosols. The authors stated that the nanomaterial-assisted PCR method lowered the detection limit of airborne biological contamination down to 40 pg/μl, which has 500 times enhanced sensitivity than conventional PCR.

Table 4: Effects of other nanoparticles on PCR

Nanomaterial	Size (nm)	[Final]	Effect	Template	Enzyme	Mg [mM]	Ref.
C_{60}	-	0.25-0.5	Improved efficiency	DNA (60 & 110 bp)	*Taq*	-	[36]
$C_{60}(OH)_{20}$	-	0.02-0.4 μM	Inhibition	HTSF gene (7 kbp)	*Taq*	2	[122]
TiO$_2$ NPs	25	0.4	Improved efficiency	Human HMGCR Exon 11 (364 bp)	*Taq*	1.5	[38]
				Human CHGA Exon 7 (534 bp)			
				Human HSPA1A pro. (1035 bp)			
				Mouse HMGCR, cDNA domain b. Exon 9 & 11 (448 bp)			
TiO$_2$ NPs	-	0.6	Improved sensitivity	Bacterial Aerosols	*Taq*	-	[124]
ZnO Tetrapods	--	1 mg/ml	Improved efficiency	pEGFPN1	*Taq*	1.6	[125]
Ag NPs	-	0.9	Improved sensitivity	Bacterial Aerosols	*Taq*	-	[124]
Pt NPs	2±0.8		Reduced reaction duration	*B*-globin (248 bp)	*Taq*+	3.5	[126]
P(NVP-co-TrpAMT) micelles	60-90	0.1 μg/ml	Improved efficiency	*B*-actin (496 bp)	*Taq*	-	[127]
G5.NH$_2$ Dendrimers	-	1.35 nM	Improved specificity and efficiency	λDNA (283 bp)	Ex *Taq*	3.5	[128]
Branched PEI	-	0.076 μg/ml	Improved specificity and efficiency	λDNA (283 bp)	Ex *Taq*	1.5	[89]

Moreover, amine and silica functionalized ZnO tetrapods have also been employed to improve PCR,[125] wherein amine-functionalized ZnO tetropods showed higher PCR efficiency compared to silica-functionalized tetrapods and control groups showing no improvement in specificity. Noble metals such as platinum (β-cyclodextrin capped) showed no improvement on PCR efficiency and specificity, however, it

provided significant improvement in sensitivity and heat transfer leading to a reduction in reaction period.[126] Furthermore, Wang and coworkers[129] reported three round enhanced PCR amplification of long DNA templates by incorporating 70 nm silver nanoparticles (AgNPs) into PCR amplification.

A small number of nanostructured polymers have also been engaged in nanomaterial-assisted PCR. Firstly, employment of amphiphilic copolymer Poly(NVP-co-TrpAMT) with a micelle size of 60-90 nm has resulted in enhanced PCR amplification of GC-rich β-actin.[127] Likewise, generation 4 and 5 poly(amidoamine) (G4 & G5 PAMAM) dendrimers have been demonstrated to be useful in both the efficiency and specificity enhancement of two round error-prone PCR of λ-DNA.[128] It has been reported that the presence of amine functional groups at higher ratios lowers the optimal concentration to as low as 1.35 nM, which is 4-fold lower concentration than the ones defined for acetylated and carboxylated dendrimers. Finally, like PAMAM dendrimers, which carry substantial amount of amine groups, branched Polyethyleneimine (PEI) polymer also exhibit significant efficiency and specificity improvement at considerably low concentrations (0.076 mg/ml).[89]

7. Executive Summary and Discussion

Nanomaterial-assisted PCR is a novel area of nanobiotechnology that integrates nanomaterials with unique properties into conventional PCR system in order to achieve superior amplification products. In this review, latest developments and progress in the field of nanomaterial-assisted PCR are evaluated with a slight focus on putative interaction mechanisms. The effects of different nanomaterials on the efficiency, specificity and fidelity of the target product are summarized and the putative interaction mechanisms between nanomaterials and key PCR components are discussed in detail.

In nanomaterial-assisted PCR, the fact revolves around conditional PCR enhancement via nanomaterials depending on their concentration, thermal conductivity, electron transfer properties, size and surface modifications. Despite several contradictory reports, key benefits of nanomaterial-assisted PCR are mainly associated with the increase in yield and specificity of the target product along with limited information on PCR fidelity. It is important to note that any indication of compromised fidelity renders other improvements irrelevant, thus, fidelity in nanomaterial-assisted PCR requires dedicated research and careful assessment. Another issue that remains ambiguous is the elimination of nanomaterials from PCR for subsequent

applications. For example, AuNPs below 20 nm in diameter would require a considerable g-force and long centrifugation period to precipitate in a solution. Their comparable size to amplicon would render filtering methods ineffective. Similarly, CNTs and graphene derivatives could be incompatible with centrifuge methods due to their similar size and density with DNA amplicon. Although gel purification methods might be one option to remove nanomaterials from the solution it would not be practical for high-throughput applications like cloning or sequencing. But CNTs can be attached onto removable surfaces for effective utilization; for example, amine functionalized CNTs can be covalently attached on carboxyl functionalized magnetic beads via NHS-EDC chemistry. Alternatively, CNT-integrated PCR tubes could be developed and superior thermal conductivities of CNTs can be utilized to construct new thermal cycler blocks. Owing to their tunable properties, it might be possible to produce novel CNTs that bear desired features for PCR enhancement while avoiding inhibiting properties.

As anticipated, each nanomaterial would display a different interaction mechanism in PCR as a consequence of their unique physical and chemical properties. Since mainstream information regarding the interaction system between PCR reagents and nanomaterials has been focused on AuNPs, specific interactions of other nanomaterials proceeding at bio-nano interface have not been understood in detail yet. Nevertheless, the following list of assumptions has been provided by considering the typical properties of nanoparticles (i.e., thermal conductivity, high surface to volume ratio, stability, water solubility), which could shed light on association of the nanomaterials with major PCR components.

- **High surface to volume ratio:** High surface to volume ratios of nanomaterials provide an excellent environment for adsorption and desorption of PCR components on nanomaterial surface. It has been well-proven in the literature that ssDNA and DNA polymerase enzyme bind on nanomaterial surface via π-π stacking, surface charge facilitated interactions or van der Waals' forces.[78,130,90,59,131] It was reported long before that AuNPs-modified with ssDNA can distinguish a perfect complementary strand from a single base mutated sequence,[132] which could rationalize the enhanced specificity in nanomaterial-assisted PCR. However, it could be wise to optimize the nanomaterial concentration so that they cannot offer a huge surface where the all reactants concentrate at once and stop reacting.

- **Vroman (like) effect:** In a complex media where different types of molecules emerge, there will be a dynamic competition among biomolecules to adsorb on the surface of nanomaterials. Most abundant

biomolecules (mainly short/small ones) will adsorb on the surface at the earlier stages, however, they will be substituted with biomolecules of lower concentration but with greater affinity (mainly larger biomolecules) over the time, which is a phenomenon called Vroman's effect.[57,133] Based on this fact, it is possible to observe a significant change in PCR efficiency upon attachment of DNA polymerase on nanomaterial surface. Depending on the DNA polymerase concentration in the solution, the change in efficiency could be in either way, thus efficiency of nano-assisted PCR could be dependent on the equilibrium kinetics of enzyme adsorption.

- **Biomolecule/Protein corona:** The term Corona refers to the adsorption of different proteins and biomolecules onto the nanoparticle surface over time depending on their size and affinities. The structure and composition of corona depends on the physicochemical aspects of the nanomaterials (size, curvature, surface charges and functional groups), temperature and duration of exposure, thus making corona unique for each nanomaterial.[134,135] Even though entropy-driven binding usually does not change the conformation of the protein,[136] it has been reported that loss of α-helical content occurs when proteins are adsorbed onto nanomaterials. For example, it has been reported that there is a 10% decrease in the alpha-helix structure of human adult hemoglobin upon binding on CdS nanoparticles via sulfur atoms of cysteine residues.[137] In this context, adsorption of DNA polymerase onto the nanomaterial surface might induce a conformational change that might modulate enzyme's activity.[62,59]

- **Surface charge of nanomaterials:** Zeta potential is an important parameter to apprehend the nanomaterial surface charge and predicting the long-term stability of the colloidal solutions. Nanomaterials with a zeta potential between -10 and +10 mV are considered as almost neutral, while zeta potentials of greater than +30 mV or less than -30 mV are assumed to be cationic and anionic, respectively.[138] Selective adsorption of biomolecules on several nanomaterials has been demonstrated previously and for numerous proteins the mechanisms of binding have been referred to the electrostatic interaction.[139,140,137] In light of these facts, it can be hypothesized that negatively charged phosphate backbones of DNA molecules would tend to condense on cationic nano surfaces rather than anionic surfaces, and likewise, kinetics of DNA polymerase would be affected from the zeta potential of the nanomaterial, which would ultimately increase the dynamic interaction between biomolecules and nanomaterials.

Consequently, the exciting interaction of nanomaterials with biomolecules provides researchers unique opportunities to proceed and design nano-based PCR additives that can be incorporated into single reactions, PCR tubes, PCR plates and thermal cyclers, so that the critical PCR complications can be addressed in a shorter, simpler and cost-effective manner that can far surpass current technologies. Nanomaterial-assisted PCR offers several advantages over traditional PCR, such as elimination of time-consuming PCR optimizations, higher efficiency and specificity for difficult GC-rich and long DNA sequences. However, reliability and accuracy of nanomaterial-assisted PCR remains in question considering limited research on the fidelity aspect and possible toxicity imposed by nanomaterials. At this point, a systematic and comprehensive approach should be followed in order to elucidate the fundamental mechanisms of nanomaterial-assisted PCR and address the demands of PCR related applications.

Acknowledgements

References

1.   K. Kleppe, E. Ohtsuka, R. Kleppe, I. Molineux, and H. G. Khorana, *J. Mol. Biol.*, 1971, **56**, 341–361.

2.   K. Mullis, F. Faloona, S. Scharf, R. Saiki, G. Horn, and H. Erlich, *Cold Spring Harb. Symp. Quant. Biol.*, 1986, **51 Pt 1**, 263–273.

3.   K. B. Mullis, *Angew. Chemie Int. Ed. English*, 1994, **33**, 1209–1213.

4.   A. Chien, D. B. Edgar, and J. M. Trela, *J. Bacteriol.*, 1976, **127**, 1550–1557.

5.   A. Hadidi, R. Flores, J. Randles, and J. Semancik, *Viroids: Properties, Detection, Diseases and their Control*, Csiro Publishing, 2003.

6.   M. Orita, Y. Suzuki, T. Sekiya, and K. Hayashi, *Genomics*, 1989, **5**, 874–879.

7.   J. N. Larsen, P. Strøman, and H. Ipsen, *Mol. Immunol.*, 1992, **29**, 703–711.

8.   J. Cheng, Y. Zhang, and Q. Li, *Nucleic Acids Res.*, 2004, **32**, e61.

9.   M. Huber, A. Mündlein, E. Dornstauder, C. Schneeberger, C. B. Tempfer, M. W. Mueller, and W. M. Schmidt, *Anal. Biochem.*, 2002, **303**, 25–33.

10.   J. Shendure and H. Ji, *Nat. Biotechnol.*, 2008, **26**, 1135–1145.

11. J. Welsh and M. McClelland, *Nucleic Acids Res.*, 1990, **18**, 7213–7218.

12. B. Rerkamnuaychoke, W. Chantratita, U. Jomsawat, J. Thanakitgosate, and P. Rojanasunan, *J. Med. Assoc. Thai.*, 2000, **83 Suppl 1**, S55–62.

13. O. Lazcka, F. J. Del Campo, and F. X. Muñoz, *Biosens. Bioelectron.*, 2007, **22**, 1205–1217.

14. K. Kasai, Y. Nakamura, and R. White, *J. Forensic Sci.*, 1990, **35**, 1196–1200.

15. S. Yang and R. E. Rothman, *Lancet Infect. Dis.*, 2004, **4**, 337–348.

16. N. Zou, S. Ditty, B. Li, and S.-C. Lo, *Biotechniques*, 2003, **35**, 758–60, 762–5.

17. R. R. Meyer and P. S. Laine, *Microbiol. Rev.*, 1990, **54**, 342–380.

18. C. M. Nagamine, K. Chan, and Y. F. Lau, *Am. J. Hum. Genet.*, 1989, **45**, 337–339.

19. A. M. Dunning, P. Talmud, and S. E. Humphries, *Nucleic Acids Res.*, 1988, **16**, 10393.

20. X. Qiu, L. Wu, H. Huang, P. E. McDonel, A. V Palumbo, J. M. Tiedje, and J. Zhou, *Appl. Environ. Microbiol.*, 2001, **67**, 880–887.

21. M. F. Polz and C. M. Cavanaugh, *Appl. Envir. Microbiol.*, 1998, **64**, 3724–3730.

22. U. H. Frey, H. S. Bachmann, J. Peters, and W. Siffert, *Nat. Protoc.*, 2008, **3**, 1312–1317.

23. K. Varadaraj and D. M. Skinner, *Gene*, 1994, **140**, 1–5.

24. G. Sarkar, S. Kapelner, and S. S. Sommer, *Nucleic Acids Res.*, 1990, **18**, 7465.

25. M. Musso, R. Bocciardi, S. Parodi, R. Ravazzolo, and I. Ceccherini, *J. Mol. Diagnostics*, 2006, **8**, 544–550.

26. M. A. Jensen, M. Fukushima, and R. W. Davis, *PLoS One*, 2010, **5**, e11024.

27. K. E. Drexler, *Anchor Books*, 1986.

28. A. E. Nel, L. Mädler, D. Velegol, T. Xia, E. M. V Hoek, P. Somasundaran, F. Klaessig, V. Castranova, and M. Thompson, *Nat. Mater.*, 2009, **8**, 543–557.

29. A. K. Geim and K. S. Novoselov, *Nat. Mater.*, 2007, **6**, 183–191.

30. S. Berber, Y. K. Kwon, and D. Tománek, *Phys. Rev. Lett.*, 2000, **84**, 4613–4616.

31. Y. C. Lin and H. L. Wu, in *Transducers 2007 - International Solid-State Sensors, Actuators and Microsystems Conference*, IEEE, 2007, pp. 391–394.

32. X. Lou and Y. Zhang, *ACS Appl. Mater. Interfaces*, 2013, **5**, 6276–6284.

33. J. Jia, L. Sun, N. Hu, G. Huang, and J. Weng, *Small*, 2012, **8**, 2011–2015.

34. L. Ma, S. He, J. Huang, L. Cao, F. Yang, and L. Li, *Biochimie*, 2009, **91**, 969–973.

35.   S.-H. Hwang, S.-G. Im, S. S. Hah, V. T. Cong, E. J. Lee, Y.-S. Lee, G. K. Lee, D.-H. Lee, and S. J. Son, *PLoS One*, 2013, **8**, e73408.

36.   Y. Liang, F. Luo, Y. Lin, Q. Zhou, and G. Jiang, *Carbon N. Y.*, 2009, **47**, 1457–1465.

37.   R. M. Williams, S. Nayeem, B. D. Dolash, and L. J. Sooter, *PLoS One*, 2014, **9**, e94117.

38.   R. Abdul Khaliq, P. J. Sonawane, B. K. Sasi, B. S. Sahu, T. Pradeep, S. K. Das, and N. R. Mahapatra, *Nanotechnology*, 2010, **21**, 255704.

39.   W. Tong, X. Cao, S. Wen, R. Guo, M. Shen, J. Wang, and X. Shi, *Int. J. Nanomedicine*, 2012, **7**, 1069–1078.

40.   P. Alivisatos, *Nat. Biotechnol.*, 2004, **22**, 47–52.

41.   N. L. Rosi and C. A. Mirkin, *Chem. Rev.*, 2005, **105**, 1547–1562.

42.   V. M. Rotello, P. Ghosh, G. Han, M. De, and C. K. Kim, *Adv. Drug Deliv. Rev.*, 2008, **60**, 1307–1315.

43.   X. Liu, Q. Dai, L. Austin, J. Coutts, G. Knowles, J. Zou, H. Chen, and Q. Huo, *J. Am. Chem. Soc.*, 2008, **130**, 2780–2782.

44.   D. Pissuwan, S. M. Valenzuela, and M. B. Cortie, *Trends Biotechnol.*, 2006, **24**, 62–67.

45.   U. H. F. Bunz and V. M. Rotello, *Angew. Chem. Int. Ed. Engl.*, 2010, **49**, 3268–3279.

46.   P. Chen, D. Pan, C. Fan, J. Chen, K. Huang, D. Wang, H. Zhang, Y. Li, G. Feng, P. Liang, L. He, and Y. Shi, *Nat. Nanotechnol.*, 2011, **6**, 639–644.

47.   H. Li, J. Huang, J. Lv, H. An, X. Zhang, Z. Zhang, C. Fan, and J. Hu, *Angew. Chem. Int. Ed. Engl.*, 2005, **44**, 5100–5103.

48.   M. Li, Y. C. Lin, C. C. Wu, and H. S. Liu, *Nucleic Acids Res.*, 2005, **33**, e184.

49.   W. Yang, L. Mi, X. Cao, X. Zhang, C. Fan, and J. Hu, *Nanotechnology*, 2008, **19**, 255101.

50.   A. L. Haber, K. R. Griffiths, A. K. Jamting, and K. R. Emslie, *Anal. Bioanal. Chem.*, 2008, **392**, 887–896.

51.   B. V. Vu, D. Litvinov, and R. C. Willson, *Anal. Chem.*, 2008, **80**, 5462–5467.

52.   S. H. Huang, T. C. Yang, M. H. Tsai, I. S. Tsai, H. C. Lu, P. H. Chuang, L. Wan, Y. J. Lin, C. H. Lai, and C. W. Lin, *Nanotechnology*, 2008, **19**, 405101.

53.   W. Yang, X. Li, J. Sun, and Z. Shao, *ACS Appl. Mater. Interfaces*, 2013, **5**, 11520–11524.

54.   P. Keblinski, S. . Phillpot, S. U. . Choi, and J. . Eastman, *Int. J. Heat Mass Transf.*, 2002, **45**, 855–863.

55.   D. Kumar, H. Patel, V. Kumar, T. Sundararajan, T. Pradeep, and S. Das, *Phys. Rev. Lett.*, 2004, **93**, 144301.

56.   W. Wan and J. T. W. Yeow, *Nanotechnology*, 2009, **20**, 325702.

57.   L. Vroman, A. L. Adams, G. C. Fischer, and P. C. Munoz, *Blood*, 1980, **55**, 156–159.

58.   Slack Steven M. and Horbett Thomas A., *Proteins at Interfaces II*, American Chemical Society, Washington, DC, 1995, vol. 602.

59.   L. Sun, S. Wang, Z. Zhang, Y. Ma, Y. Lai, J. Weng, and Q. Zhang, *IET Nanobiotechnol.*, 2011, **5**, 20–24.

60.   L. Mi, Y. Wen, D. Pan, Y. Wang, C. Fan, and J. Hu, *Small*, 2009, **5**, 2597–2600.

61.   C. Shen, W. Yang, Q. Ji, H. Maki, A. Dong, and Z. Zhang, *Nanotechnology*, 2009, **20**, 455103.

62.   S. Mandal, M. Hossain, T. Muruganandan, G. S. Kumar, and K. Chaudhuri, *RSC Adv.*, 2013, **3**, 20793–20799.

63.   H. Li and L. Rothberg, *Proc. Natl. Acad. Sci. U. S. A.*, 2004, **101**, 14036–14039.

64.   E. M. Nelson and L. J. Rothberg, *Langmuir*, 2011, **27**, 1770–1707.

65.   H. Li and L. J. Rothberg, *J. Am. Chem. Soc.*, 2004, **126**, 10958–10961.

66.   J. Chen, X. Cao, R. Guo, M. Shen, C. Peng, T. Xiao, and X. Shi, *Analyst*, 2012, **137**, 223–228.

67.   L. Yuan and Y. He, *Analyst*, 2013, **138**, 539–545.

68.   H. Kimura-Suda, D. Y. Petrovykh, M. J. Tarlov, and L. J. Whitman, *J. Am. Chem. Soc.*, 2003, **125**, 9014–9015.

69.   W. Yang, K. R. Ratinac, S. P. Ringer, P. Thordarson, J. J. Gooding, and F. Braet, *Angew. Chem. Int. Ed. Engl.*, 2010, **49**, 2114–2138.

70.   J. Z. Liao and M. J. Tan, *Adv. Mater. Res.*, 2012, **500**, 651–656.

71.   S. Iijima and T. Ichihashi, *Nature*, 1993, **363**, 603–605.

72.   G. Che, B. B. Lakshmi, E. R. Fisher, and C. R. Martin, *Nature*, 1998, **393**, 346–349.

73.   W. A. de Heer, A. Chetelain, and D. Ugarte, *Science (80-.).*, 1995, **270**, 1179–1180.

74.   C. Staii, A. T. Johnson, M. Chen, and A. Gelperin, *Nano Lett.*, 2005, **5**, 1774–1778.

75.   H. Dai, J. H. Hafner, A. G. Rinzler, D. T. Colbert, and R. E. Smalley, *Nature*, 1996, **384**, 147–150.

76.   L. Minati, V. Antonini, M. Dalla Serra, and G. Speranza, *Langmuir*, 2012, **28**, 15900–15906.

77.   H. Nie, Z. Yang, S. Huang, Z. Wu, H. Wang, R. Yu, and J. Jiang, *Small*, 2012, **8**, 1407–1414.

78.   M. Zheng, A. Jagota, E. D. Semke, B. A. Diner, R. S. McLean, S. R. Lustig, R. E. Richardson, and N. G. Tassi, *Nat. Mater.*, 2003, **2**, 338–342.

79.   C. R. Martin and P. Kohli, *Nat. Rev. Drug Discov.*, 2003, **2**, 29–37.

80.   D. Cui, F. Tian, Y. Kong, I. Titushikin, and H. Gao, *Nanotechnology*, 2004, **15**, 154–157.

81.   H. R. Marsden, L. Gabrielli, and A. Kros, *Polym. Chem.*, 2010, **1**, 1512–1518.

82.   G. M. Whitesides and M. Boncheva, *Proc. Natl. Acad. Sci. U. S. A.*, 2002, **99**, 4769–4774.

83.   Z. Zhang, C. Shen, M. Wang, H. Han, and X. Cao, *Biotechniques*, 2008, **44**, 537–545.

84.   J. Hone, M. Whitney, C. Piskoti, and A. Zettl, *Phys. Rev. B*, 1999, **59**, 2514–2516.

85.   A. K. Hüttel, G. A. Steele, B. Witkamp, M. Poot, L. P. Kouwenhoven, and H. S. J. van der Zant, *Nano Lett.*, 2009, **9**, 2547–2552.

86.   M. Fujii, X. Zhang, H. Xie, H. Ago, K. Takahashi, T. Ikuta, H. Abe, and T. Shimizu, *Phys. Rev. Lett.*, 2005, **95**, 65502.

87.   M. L. V. Ramires, C. A. Nieto de Castro, Y. Nagasaka, A. Nagashima, M. J. Assael, and W. A. Wakeham, *J. Phys. Chem. Ref. Data*, 1995, **24**, 1377–1381.

88.   M. Quaglio, S. Bianco, R. Castagna, M. Cocuzza, and C. F. Pirri, *Microelectron. Eng.*, 2011, **88**, 1860–1863.

89.   X. Cao, J. Chen, S. Wen, C. Peng, M. Shen, and X. Shi, *Nanoscale*, 2011, **3**, 1741–1747.

90.   C. Yi, C.-C. Fong, W. Chen, S. Qi, C.-H. Tzang, S.-T. Lee, and M. Yang, *Nanotechnology*, 2007, **18**, 025102.

91.   S. Kang, M. Herzberg, D. F. Rodrigues, and M. Elimelech, *Langmuir*, 2008, **24**, 6409–6413.

92.   I. Fenoglio, M. Tomatis, D. Lison, J. Muller, A. Fonseca, J. B. Nagy, and B. Fubini, *Free Radic. Biol. Med.*, 2006, **40**, 1227–1233.

93.   J.-S. Lauret, C. Voisin, G. Cassabois, C. Delalande, P. Roussignol, O. Jost, and L. Capes, *Phys. Rev. Lett.*, 2003, **90**, 057404.

94.   J. Yu, N. Grossiord, C. E. Koning, and J. Loos, *Carbon N. Y.*, 2007, **45**, 618–623.

95.   W. S. Hummers and R. E. Offeman, *J. Am. Chem. Soc.*, 1958, **80**, 1339–1339.

96.   H. Shen, M. Hu, Z. Yang, C. Wang, and L. Zhu, *Chinese Sci. Bull.*, 2013, **50**, 2016–2020.

97.   D. Chen, H. Feng, and J. Li, *Chem. Rev.*, 2012, **112**, 6027–6053.

98.   L. Liu, J. Zhang, J. Zhao, and F. Liu, *Nanoscale*, 2012, **4**, 5910–5916.

99.   S. Li, A. N. Aphale, I. G. Macwan, P. K. Patra, W. G. Gonzalez, J. Miksovska, and R. M. Leblanc, *ACS Appl. Mater. Interfaces*, 2012, **4**, 7069–7075.

100. C. Chung, Y. Kim, D. Shin, S.-R. Ryoo, B. H. E. E. Hong, and D.-H. Min, *Acc. Chem. Res.*, 2013, **46**, 2211–2224.

101. C. Mattevi, G. Eda, S. Agnoli, S. Miller, K. A. Mkhoyan, O. Celik, D. Mastrogiovanni, G. Granozzi, E. Garfunkel, and M. Chhowalla, *Adv. Funct. Mater.*, 2009, **19**, 2577–2583.

102. Y. Wang, Z. Li, J. Wang, J. Li, and Y. Lin, *Trends Biotechnol.*, 2011, **29**, 205–212.

103. R. Abdul Khaliq, R. M. Kafafy, H. M. Salleh, and W. F. Faris, *Nanotechnology*, 2012, **23**, 455106.

104. T. Le, E. H. Ashrafi, N. Paul, and E. Hidalgo Ashrafi, *Biotechniques*, 2009, **47**, 972–973.

105. S. He, B. Song, D. Li, C. Zhu, W. Qi, Y. Wen, L. Wang, S. Song, H. Fang, and C. Fan, *Adv. Funct. Mater.*, 2010, **20**, 453–459.

106. A. A. Balandin, S. Ghosh, W. Bao, I. Calizo, D. Teweldebrhan, F. Miao, and C. N. Lau, *Nano Lett.*, 2008, **8**, 902–907.

107. Y. Liu, Y. Luo, J. Wu, Y. Wang, X. Yang, R. Yang, B. Wang, J. Yang, and N. Zhang, *Sci. Rep.*, 2013, **3**, 3469.

108. S. Liu, T. H. Zeng, M. Hofmann, E. Burcombe, J. Wei, R. Jiang, J. Kong, and Y. Chen, *ACS Nano*, 2011, **5**, 6971–6980.

109. O. Akhavan and E. Ghaderi, *ACS Nano*, 2010, **4**, 5731–5736.

110. T. R. Nayak, H. Andersen, V. S. Makam, C. Khaw, S. Bae, X. Xu, P.-L. R. Ee, J.-H. Ahn, B. H. Hong, G. Pastorin, and B. Özyilmaz, *ACS Nano*, 2011, **5**, 4670–4678.

111. S. Pathak, S. K. Choi, N. Arnheim, and M. E. Thompson, *J. Am. Chem. Soc.*, 2001, **123**, 4103–4104.

112. B. Dubertret, P. Skourides, D. J. Norris, V. Noireaux, A. H. Brivanlou, and A. Libchaber, *Science*, 2002, **298**, 1759–1762.

113. L. Chen, A. J. Zurita, P. U. Ardelt, R. J. Giordano, W. Arap, and R. Pasqualini, *Chem. Biol.*, 2004, **11**, 1081–1091.

114. L. Y. Lee, S. L. Ong, J. Y. Hu, W. J. Ng, Y. Feng, X. Tan, and S. W. Wong, *Appl. Environ. Microbiol.*, 2004, **70**, 5732–5736.

115. G. Liang, C. Ma, Y. Zhu, S. Li, Y. Shao, Y. Wang, and Z. Xiao, *Nanoscale Res. Lett.*, 2010, **6**, 51.

116. L. Wang, Y. Zhu, Y. Jiang, R. Qiao, S. Zhu, W. Chen, and C. Xu, *J. Phys. Chem. B*, 2009, **113**, 7637–7641.

117. F. Sang, *J. Biomed. Sci. Eng.*, 2012, **05**, 295–301.

118. Z. Xun, X. Zhao, and Y. Guan, *Nanotechnology*, 2013, **24**, 355504.

119. F. Sang, Z. Zhang, Z. Xu, X. Ju, H. Wang, S. Zhang, and C. Guo, *Mol. Biotechnol.*, 2013, **54**, 969–976.

120. F. Sang, Y. Yang, H. Zhao, M. Ma, and Z. Zhang, *J. Exp. Nanosci.*, 2013, 1–7.

121. Q. Chou, *Nucleic Acids Res.*, 1992, **20**, 4371.

122. J. Shang, T. A. Ratnikova, S. Anttalainen, E. Salonen, P. C. Ke, and H. T. Knap, *Nanotechnology*, 2009, **20**, 415101.

123. P. Nedumpully Govindan, L. Monticelli, and E. Salonen, *J. Phys. Chem. B*, 2012, **116**, 10676–10683.

124. S. Xu and M. Yao, *J. Aerosol Sci.*, 2013, **65**, 1–9.

125.   L. Nie, L. Gao, X. Yan, and T. Wang, *Nanotechnology*, 2007, **18**, 015101.

126.   S. Petralia, T. Barbuzzi, and G. Ventimiglia, *Mater. Sci. Eng. C*, 2012, **32**, 848–850.

127.   L. Zhang, Y. Liang, L. Meng, X. Lu, and Y. Liu, *Chem. Biodivers.*, 2007, **4**, 163–174.

128.   X. Cao, X. Shi, W. Yang, X. Zhang, C. Fan, and J. Hu, *Analyst*, 2009, **134**, 87–92.

129.   Q. Wang, J. Li, X. Cao, and Z. Zhang, *J. Tianjin Univ. Sci. Technol.*, 2007, 1–5.

130.   C. H. Lu, H. H. Yang, C. L. Zhu, X. Chen, and G. N. Chen, *Angew. Chemie*, 2009, **121**, 4879–4881.

131.   E. Uysal, M. Yuce, and H. Kurt, *N. Biotechnol.*, 2014.

132.   J. J. Storhoff, R. Elghanian, R. C. Mucic, C. A. Mirkin, and R. L. Letsinger, *J. Am. Chem. Soc.*, 1998, **120**, 1959–1964.

133.   D. Y. Furgeson, M. A. Dobrovolskaia, P. Aggarwal, J. B. Hall, C. B. McLeland, M. A. Dobrovolskaia, and S. E. McNeil, *Adv. Drug Deliv. Rev.*, 2009, **61**, 428–437.

134.   M. Lundqvist, *Nat. Nanotechnol.*, 2013, **8**, 701–702.

135.   P. del Pino, B. Pelaz, Q. Zhang, P. Maffre, G. U. Nienhaus, and W. J. Parak, *Mater. Horizons*, 2014.

136.   M. Rahman, S. Laurent, N. Tawil, L. Yahia, and M. Mahmoudi, *Protein-Nanoparticle Interactions: The Bio-Nano Interface (Google eBook)*, Springer Science & Business, 2013.

137.   I. Lynch and K. A. Dawson, *Nano Today*, 2008, **3**, 40–47.

138.   J. D. Clogston and A. K. Patri, *Methods Mol. Biol.*, 2011, **697**, 63–70.

139.   H.-Q. Mao, K. Roy, V. L. Troung-Le, K. A. Janes, K. Y. Lin, Y. Wang, J. T. August, and K. W. Leong, *J. Control. Release*, 2001, **70**, 399–421.

140.   M. N. V. Ravi Kumar, U. Bakowsky, and C. M. Lehr, *Biomaterials*, 2004, **25**, 1771–1777.